

1     **Glycogen metabolism jump-starts photosynthesis through the oxidative pentose phosphate**  
2   **pathway (OPPP) in cyanobacteria**

3     Shrameeta Shinde<sup>1</sup>, Sonali P. Singapuri<sup>1</sup>, Xiaohui Zhang<sup>1,2</sup>, Isha Kalra<sup>1</sup>, Xianhua Liu<sup>2</sup>, Rachael  
4   M. Morgan-Kiss<sup>1</sup>, and Xin Wang<sup>1\*</sup>

5  
6     <sup>1</sup>Department of Microbiology, Miami University, Oxford OH 45056

7     <sup>2</sup>School of Environmental Science and Engineering, Tianjin University, Tianjin, 300354, China

8

9     **Keywords:**   Photosynthesis; Glycogen metabolism; G6P shunt; oxidative pentose phosphate  
10    pathway; cyanobacteria

11

12    \*Correspondence:

13    **Xin Wang:** xwang@miamioh.edu | 513.529.5427

## 1 **Abstract**

2           Cyanobacteria experience drastic changes in their carbon metabolism under daily light-  
3 dark cycles. In the light, the Calvin-Benson cycle fixes CO<sub>2</sub> and divert excess carbon into  
4 glycogen storage. At night, glycogen is degraded to support cellular respiration. Dark-light  
5 transition represents a universal environmental stress for cyanobacteria and other photosynthetic  
6 lifeforms. Recent studies in the field revealed the essential genetic background necessary for the  
7 fitness of cyanobacteria during diurnal growth. However, the metabolic engagement behind the  
8 dark-light transition is not well understood. In this study, we discovered that glycogen  
9 metabolism can jump-start photosynthesis in the cyanobacterium *Synechococcus elongatus* PCC  
10 7942 when photosynthesis reactions start upon light. Compared to the wild type, the glycogen  
11 mutant ( $\Delta$ *lgC*) showed much lower photosystem II efficiency and slower photosystem I-  
12 mediated cyclic electron flow rate when photosynthesis starts. Proteomics analyses indicated that  
13 glycogen is degraded through the oxidative pentose phosphate pathway (OPPP) during dark-light  
14 transition. We confirmed that the OPPP is essential for the initiation of photosynthesis, and  
15 further showed that glycogen degradation through the OPPP is likely to contribute to the  
16 activation of key Calvin-Benson cycle enzymes by modulating NADPH levels during the  
17 transition period. This ingenious strategy helps jump-start photosynthesis in cyanobacteria  
18 following dark respiration, and stabilize the Calvin-Benson cycle under fluctuating  
19 environmental conditions. It has evolutionary advantages for the survival of photosynthetic  
20 organisms using the Calvin-Benson cycle for carbon fixation.

## 1 **Introduction**

2           Photosynthesis supports life on earth by converting solar energy into chemical energy  
3 stored as organic carbon. The Calvin-Benson cycle, the major carbon fixation pathway in  
4 cyanobacteria, algae and plants, is employed to reduce CO<sub>2</sub> into organic carbon molecules. Since  
5 its discovery in the 1950s, the enzymes of the Calvin-Benson cycle have been elucidated and  
6 consensus pathways established (Bassham et al., 1954). CO<sub>2</sub> is reduced into the photosynthesis  
7 output glyceraldehyde 3-phosphate (G3P) in three stages, i.e. carbon fixation, carbon reduction,  
8 and carbon regeneration. The Calvin-Benson cycle is an elegant pathway that the starting  
9 substrate ribulose 1,5-bisphosphate (RuBP) is continuously supplied by partially recycling G3P  
10 back to RuBP through carbon rearrangement reactions. This carbon regeneration stage resembles  
11 the non-oxidative portion of the pentose phosphate pathway but with key differences. A key  
12 enzyme sedoheptulose-1,7-bisphosphatase (SBPase) was evolutionally selected to drive the  
13 carbon regeneration in the Calvin-Benson cycle rather than using the transaldolase found in the  
14 pentose phosphate pathway(Sharkey and Weise, 2016). The activity of SBPase often determines  
15 the photosynthetic capacity and carbon accumulation in downstream metabolic  
16 processes(Harrison et al., 1997; Raines et al., 1999; Harrison et al., 2001).

17           In cyanobacteria, a major portion of the photosynthesis-fixed carbon is used to synthesize  
18 the storage carbon glycogen. Two enzymes, ADP-glucose pyrophosphorylase (AGPase) and  
19 glycogen synthase (GS), catalyze the sequential conversion of glucose-1-phosphate (G1P) to 1,4-  
20 alpha-glucan (Preiss, 1984). Another enzyme encoded by 1,4-alpha-glucan-branching enzyme  
21 gene, *glgB*, can catalyze the formation of the 1,6-alpha branches of glycogen(Preiss, 1984).  
22 Glycogen synthesis is closely linked to photosynthesis carbon output. The photosynthate 3-  
23 phosphoglycerate (PGA) is an allosteric activator of the AGPase (Preiss, 1984; Gomez-Casati et

1 al., 2003). When photosynthesis fixed carbon is in excess, a major carbon flux will be diverted to  
2 glycogen storage, which will serve as the carbon and electron sources for cellular respiration in  
3 the dark(Preiss, 1984; Suzuki et al., 2010). More recently, glycogen metabolism has also been  
4 recognized for additional roles played in cyanobacterial carbon metabolism. These studies  
5 revealed the involvement of glycogen metabolism as an energy buffering system to maintain  
6 homeostasis(Cano et al., 2018), and as the carbon source for rapid resuscitation from nitrogen  
7 chlorosis(Doello et al., 2018).

8         Glycogen metabolism and cellular respiration are critical for cell viability in the dark  
9 until light resumes(Lehmann and Wöber, 1976). Research in the past has identified the oxidative  
10 pentose phosphate (OPP) pathway, a.k.a. the glucose 6-phosphate (G6P) shunt, as the major  
11 route for glycogen degradation in the dark(Smith, 1983; Broedel and Wolf, 1990). On the other  
12 hand, the OPP pathway seems to become indispensable only after long period of dark (over 24  
13 hours), while glycolysis might have been able to compensate for the need of reducing equivalent  
14 during short incubation in the dark(Scanlan et al., 1995). However, it is also important to know  
15 that OPP pathway is responsible for generating NADPH to serve as cofactors for certain ROS-  
16 detoxifying enzymes important for cyanobacterial survival(Welkie et al., 2018). In addition,  
17 cellular respiration is closely associated with photosynthesis. Many intermediates are shared  
18 between the carbon fixation and respiration processes. In cyanobacteria, many electron carriers  
19 in the thylakoid membrane are also shared between photosynthesis light reactions and cellular  
20 respiration(Mullineaux, 2014). When photosynthesis reactions start upon light, intermediates in  
21 the Calvin-Benson cycle might be limited after dark respiration, leading to stalled carbon fixation  
22 reactions. Dynamic metabolic regulation to ensure smooth transition from dark respiration to  
23 photosynthesis reactions is thus essential for the fitness of cyanobacteria during diurnal

1 growth(Puszynska and O'Shea, 2017; Welkie et al., 2018). In this study, we discovered the active  
2 participation of glycogen metabolism during the dark-to-light transition period in cyanobacteria.  
3 We found that glycogen degradation through the OPP pathway helps activate and stabilize the  
4 Calvin-Benson cycle reactions when photosynthesis reactions start upon light. We propose that  
5 this ingenious strategy helps support photosynthesis during dark-to-light transition, and ensures  
6 the growth advantage of photosynthetic organisms in their natural environment.

## 7 **Results**

### 8 **Proteomics analysis suggests a supportive role of glycogen metabolism for photosynthesis**

9 Glycogen biosynthesis is a major carbon assimilatory pathway in the cyanobacterium  
10 *Synechococcus elongatus* PCC 7942. In this study, we generated a glycogen synthesis mutant by  
11 knocking out the AGPase gene (*glgC*) in the *S. elongatus* genome (Fig. 1A). When wild type and  
12 glycogen mutant cells were grown under moderate light levels ( $50 \mu\text{mol photons m}^{-2} \text{s}^{-1}$ ), the  
13 glycogen mutant exhibited a longer lag phase relative to wild type cells (Fig. 1B). This  
14 observation in the wild type cells suggests that glycogen metabolism might play a supportive role  
15 for the rapid photosynthesis start, i.e. a short lag phase to quickly start the carbon fixation  
16 process.

17 To understand how glycogen biosynthesis supports photosynthesis, we conducted a  
18 comparative proteomics analysis on the wild type and glycogen mutant cells. The AGPase was  
19 not detected in the glycogen mutant cells, showing the success of constructing a clean glycogen  
20 mutant. All three enzymes related to glycogen synthesis, i.e. AGPase (*glgC*), glycogen synthase  
21 (*glgA*) and 1,4-alpha-glucan branching enzyme (*glgB*), were found to be expressed significantly  
22 higher in the wild type compared with those of glycogen mutant cells (Fig. 1C). Interestingly,  
23 enzymes related to glycogen degradation were also found to be more abundant in wild type cells.

1 The alpha-1,4-glucan phosphorylase (*glgP*) that removes glucose from the glycogen chain was  
2 expressed over 4-fold higher in wild type cells (Fig. 1C and Table S1). However, if glycogen  
3 degradation were to continue through the glycolytic Embden-Meyerhof-Parnas (EMP) pathway,  
4 it would be a futile cycle to the carbon fixation pathway. We hypothesize that the glycogen  
5 hydrolysis might proceed through other alternative glycolytic pathways to support the rapid  
6 photosynthesis start in wild type cells. We began to test our hypothesis by determining the  
7 impact of abolished glycogen synthesis on photosynthetic function.

### 8 **The glycogen mutant has lower PSII efficiency when photosynthesis first starts**

9 To test our theory that glycogen metabolism can support a higher photosynthesis  
10 efficiency when photosynthesis first starts, we measured the photosystem II (PSII) efficiency  
11 using the Phyto PAM II Walz fluorometer. When cyanobacterial cells were grown under  
12 continuous light, the maximum PSII efficiency ( $F_V/F_M$ ) of wild type cells were relatively low in  
13 the first few hours of growth but gradually reached above 0.4, consistent with values reported for  
14 cyanobacteria (Campbell et al., 1998). The effective PSII efficiency ( $\Phi_{II}$ ) exhibited a similar  
15 trend, with a measured efficiency ranging from 0.25 to 0.35 in the first 20 hours growing under  
16 continuous light conditions (Fig. 2A). Interestingly, the  $\Phi_{II}$  of the glycogen mutant was  
17 significantly lower than that of wild type cells in the beginning of the growth phase, and only  
18 rose to a comparable level to the wild type cells at the later stage of growth (Fig. 2A). Thus, the  
19 differential levels of  $\Phi_{II}$  between the wild type and glycogen mutant during the lag phase  
20 confirmed our hypothesis that glycogen biosynthesis has a supportive role for photosynthesis in  
21 *S. elongatus* when photosynthesis first starts.

22 To further validate the supportive role of glycogen metabolism in starting photosynthesis,  
23 we monitored  $\Phi_{II}$  following prolonged dark incubation. Cellular respiration in the dark consumes

1 the Calvin-Benson cycle intermediates, and gradually lowers or depletes the C<sub>6</sub>, C<sub>5</sub> and C<sub>3</sub> sugar  
2 intermediates pool(Iijima et al., 2015; Diamond et al., 2017). Without the support from glycogen  
3 metabolism, we thus should observe a lower photosynthetic efficiency in glycogen mutant cells  
4 when photosynthesis restarts after the light cycle resumes. To ensure the depletion of phosphate  
5 sugars, we incubated cells in dark for 30 hours. Following the dark incubation, the  $\Phi_{II}$  was  
6 significantly higher in the wild type compared to the glycogen mutant cells during the first few  
7 hours of light (Fig. 2B), suggesting that PSII is transiently downregulated in the glycogen  
8 mutant. This result supports our hypothesis on the role of glycogen metabolism in sustaining a  
9 rapid start of photosynthesis.

#### 10 **Photosystem I-mediated cyclic electron flow (CEF) is lower in the glycogen mutant**

11 If the glycogen degradation goes through the alternative OPP pathway, there would be a  
12 higher ATP/NADPH ratio requirement during carbon fixation(Sharkey and Weise, 2016). Cyclic  
13 electron flow (CEF) around photosystem I (PSI) contributes largely to additional ATP  
14 requirements in cyanobacterial carbon metabolism(Mullineaux, 2014). We thus measured the  
15 CEF rate through P700 photooxidation under far-red (FR) light(Klughammer and Schreiber,  
16 1994; Cook et al., 2019). Oxidized PSI (P700<sup>+</sup>) absorbs strongly at wavelengths between 810-  
17 820 nm (A<sub>820</sub>), while reduced P700 has minimal absorbance at this range. Both wild type and  
18 glycogen mutant cells exhibited a rapid increase in A<sub>820</sub> after the FR light was turned on,  
19 indicating the oxidation of PSI (P700 to P700<sup>+</sup>). Once a stable A<sub>820</sub> was attained, the FR was  
20 turned off, and the rate of re-reduction of P700<sup>+</sup> to P700 ( $t_{1/2}^{red}$ ) was calculated as an estimate of  
21 P700<sup>+</sup> re-reduction from alternative electron donors, of which CEF is the major pathway(Xu et  
22 al., 1994). We monitored CEF rates in wild type and glycogen mutant cultures under both dark  
23 and light conditions. P700 kinetics was monitored in log-phase *S. elongatus* wild type and

1 glycogen mutant cells both at the end of dark incubation and after light was turned on for 2 hours  
2 and 24 hours. The ratio of  $\Delta A_{820}/A_{820}$  was comparable for both strains under all conditions (Fig.  
3 3), indicating that, unlike PSII, the amount of photooxidizable P700 was not affected by the  
4 mutation in the glycogen synthesis pathway. After dark incubation for 16 hours, both the wild  
5 type and glycogen mutant cells exhibited relatively slow  $t_{1/2}^{\text{red}}$ , suggesting that CEF is low in the  
6 cyanobacterial cultures following dark incubation (Fig. 3). However, the wild type cells  
7 exhibited more than a 2-fold faster  $t_{1/2}^{\text{red}}$  after 2 hours of incubation in the light. After 24 hours  
8 into the light, the  $t_{1/2}^{\text{red}}$  of both the wild type and glycogen mutant recovered to comparable levels  
9 (Fig. 3).

## 10 **Glycogen metabolism jump-starts photosynthesis through the oxidative pentose phosphate** 11 **pathway**

12 To determine how glycogen metabolism can help jump-start photosynthesis, we  
13 conducted another comparative proteomics study on dark-incubated cyanobacterial cells. Log-  
14 phase wild type and glycogen mutant cells were dark incubated for 16 hours before the light was  
15 turned on. After two hours into the light, cells were collected for proteomics analysis. Similar to  
16 log-phase cells collected under continuous light, the enzymes for glycogen metabolism, i.e.  
17 AGPase (*glgC*), glycogen synthase (*glgA*), 1,4-alpha-glucan branching enzyme (*glgB*), and  
18 alpha-1,4-glucan phosphorylase (*glgP*), were found in significantly higher abundances in wild  
19 type cells compared to those of glycogen mutant cells (Fig. 4A). Interestingly, the enzyme 6-  
20 phosphogluconate dehydrogenase (*gnd*), a key enzyme of the OPP pathway, was also expressed  
21 significantly higher in wild type cells (Fig. 4A). The proteomics analysis indicates that the  
22 glycogen degradation might proceed through the alternative OPP pathway.



1 To validate the involvement of the OPP pathway in stimulating a rapid photosynthesis  
2 start, we generated an OPP pathway mutant strain ( $\Delta gnd$ ) by deleting the 6-phosphogluconate  
3 dehydrogenase gene (*gnd*) in the *S. elongatus* genome. The selection of *gnd* over the G6P  
4 dehydrogenase gene (*zwf*) for the deletion is to minimize the potential impact on other metabolic  
5 process such as the Entner-Doudoroff pathway in need of the G6P dehydrogenase to  
6 proceed(Chen et al., 2016). Similar to the glycogen mutant cells, the  $\Delta gnd$  strain showed  
7 impaired growth compared to wild type cells when photosynthesis starts (Fig. 4B). We further  
8 measured the P700<sup>+</sup> re-reduction rate of the  $\Delta gnd$  cells. The wild type and  $\Delta gnd$  cells were  
9 grown to log phase under moderate light levels ( $50 \mu\text{mol photons m}^{-2} \text{s}^{-1}$ ) before the light was  
10 turn off for 16 hours. Following transition to light, the P700<sup>+</sup> re-reduction rates of both wild type  
11 and  $\Delta gnd$  cells were slow after dark incubation (Fig. 4B). However, the  $t_{1/2}^{\text{red}}$  of wild type cells  
12 quickly recovered after 2 hours of incubation in the light, whereas the  $t_{1/2}^{\text{red}}$  of the  $\Delta gnd$  cells was  
13 significantly slower (Fig. 4B). Even after 24 hours in light, the  $t_{1/2}^{\text{red}}$  of the  $\Delta gnd$  cells was still  
14 relatively slow compared to wild type cells, indicating long-term downregulation of  
15 photosynthesis (Fig. 4B). This observation confirms our hypothesis that the OPP pathway is  
16 crucial for the rapid photosynthesis start after dark incubation, and the healthy performance of  
17 photosynthesis in the light.

### 18 **The OPP pathway modulates the NADP(H)/NAD(H) levels to activate the Calvin-Benson** 19 **cycle**

20 Upon restarting of photosynthesis reactions following dark incubation, the intermediates  
21 pool needed to regenerate RuBP in the Calvin-Benson cycle may be limited or depleted(Iijima et  
22 al., 2015), leading to inferior photosynthesis performance and downregulation of the  
23 photosynthetic electron transport chain. Thus, continuous supply of RuBP during the dark-light

1 transition is likely critical for maintaining homeostatic balance between energy production by the  
2 light reactions and energy consumption by the Calvin-Benson cycle. The obvious outcome for  
3 the glycogen degradation through the OPPP is to replenish C<sub>5</sub> carbon pools. Ru5P derived from  
4 the OPP pathway can then be phosphorylated to RuBP by the phosphoribulokinase (PRK),  
5 replenishing the starting substrate for RuBisCO to continuously fix CO<sub>2</sub> in the Calvin-Benson  
6 cycle. However, PRK is inactive in the dark and requires redox regulation to become  
7 active (Tamoi et al., 2005). To validate whether the OPP pathway help activate photosynthesis,  
8 we measured the levels of reducing equivalents in wild type and glycogen mutant cells following  
9 dark incubation and after light was turned on for two hours. When photosynthesis reactions  
10 restart after dark incubation, the NADP(H)/NAD(H) ratio was significantly higher in the wild  
11 type than the glycogen mutant cells (Fig. 4C), supporting our hypothesis that glycogen  
12 metabolism through the OPP pathway can help activate the Calvin-Benson cycle for a rapid start  
13 of photosynthesis.

## 14 **Discussion**

15 Photosynthetic organisms experience drastic changes in their carbon metabolism during  
16 diurnal growth. Recent research has highlighted the contribution of glycogen metabolism and the  
17 OPP pathway to the fitness of cyanobacteria during diurnal growth (Diamond et al., 2017;  
18 Puszynska and O'Shea, 2017; Welkie et al., 2018). However, knowledge on metabolic  
19 engagement during the initiation of photosynthesis is not well understood. This study emphasizes  
20 the active role played by the glycogen metabolism and the OPP pathway when photosynthesis  
21 starts after dark respiration. Our results indicate that this supportive role is likely essential for the  
22 survival of cyanobacteria in their natural environment.

1 Cellular respiration from glycogen degradation helps maintain the cell integrity in dark.  
2 When light resumes, many enzymes for cellular respiration are inactivated, shifting cell  
3 metabolism to carbon fixation(Udvardy et al., 1984; Gleason, 1996; Sharkey and Weise, 2016).  
4 However, several recent studies have shown that cellular respiration might play more important  
5 roles than just maintaining cell viability for dark survival. A glycogen phosphorylase ( $\Delta glgP$ )  
6 mutant of *Synechocystis* sp. PCC 6803 retards dark respiration of glycogen, and had a much  
7 lower photosynthetic oxygen evolution rate(Shimakawa et al., 2014). Another study conducted in  
8 the glycogen mutant  $\Delta glgC$  of *Synechocystis* sp. PCC 6803 also exhibited a delayed activation of  
9 the Calvin-Benson cycle, and diminished photochemical efficiency when cultured under high  
10 carbon conditions(Holland et al., 2016). These studies indicate a tight link between respiration  
11 and the photosynthesis initiation process. In this study, we showed that glycogen metabolism can  
12 recharge photosynthesis through the OPP pathway in the unicellular cyanobacterium *S. elongatus*  
13 when photosynthesis reactions start upon light (Fig. 4). When light resumes after dark  
14 incubation, RuBP concentration is low due to the suppressed PRK activity in the dark(Tamoi et  
15 al., 2005). This alternative carbon flow is thus essential to stabilize photosynthesis when triose  
16 phosphate (TP) levels are insufficient to replenish RuBP through the Calvin-Benson cycle during  
17 the start of photosynthesis. The importance of the OPP pathway is further manifested by the lack  
18 of efficiency to synthesize TPs through glycogen degradation via phosphofructokinase (PFK)  
19 and phosphoglucoisomerase (PGI), both of which require high level of substrate(Knowles and  
20 Plaxton, 2003; Preiser et al., 2018). Glycogen metabolism thus serves as a perfect buffering  
21 system to supply G6P to the shunt by sensing the photosynthesis output PGA accumulation  
22 under the condition of stalled Calvin-Benson cycle reactions(Gomez-Casati et al., 2003). In  
23 addition, our proteomics results also showed that the transaldolase (*tal*), a non-essential enzyme

1 in the reductive phase of the pentose phosphate pathway, was expressed significantly higher in  
2 the wild type compared to the glycogen mutant cells when photosynthesis reactions first start  
3 (Table S1). This result suggests an underappreciated role for transaldolase during the operation  
4 of the OPPP. Interestingly, a recent genome-wide fitness study in *S. elongatus* showed similar  
5 result that the *tal* mutant was sensitive to light-dark cycles(Welkie et al., 2018).

6 Our findings echoes with the proposed mechanism by Sharkey et al. for the involvement  
7 of the OPP pathway to stabilize photosynthesis in plants(Sharkey and Weise, 2016). Sharkey  
8 suggested that the OPP pathway (a.k.a. G6P shunt) could account for 10-20% of Rubisco  
9 activity, and the enzyme SBPase plays an important role in controlling the carbon flow between  
10 the Calvin-Benson cycle and the shunt(Sharkey and Weise, 2016). Their recent evidence showed  
11 that G6P shunt was activated in a photorespiration mutant of *Arabidopsis thaliana* in which the  
12 activity of triose phosphate isomerase (TPI) was inhibited(Li et al., 2018). TPI is responsible for  
13 interconverting G3P and dihydroxyacetone phosphate (DHAP), a key reaction for RuBP  
14 regeneration in the Calvin-Benson cycle. During photosynthesis, it is critical that RuBP can be  
15 continuously regenerated for CO<sub>2</sub> fixation, which limits the carbon regeneration reactions to a  
16 small margin of error in order to maintain the stable operation of photosynthesis. Perturbation to  
17 the carbon regeneration stage of the Calvin-Benson cycle such as the TPI inhibition would lead  
18 to a temporarily impaired Calvin-Benson cycle. An alternative mechanism such as the G6P shunt  
19 is thus essential to stabilize photosynthesis.

20 The operation of the OPPP during the start of photosynthesis was revealed by the energy  
21 generation from photosynthetic light reactions. Compared to the wild type, the PSII efficiency in  
22 the glycogen mutant was significantly lower when photosynthesis starts (Fig. 3), suggesting that  
23 PSII is likely downregulated through a feedback mechanism in the glycogen mutant. We also

1 observed different P700<sup>+</sup> re-reduction rates in the wild type compared to both mutant strains  
2 ( $\Delta glgC$  and  $\Delta gnd$ ). Both wild type and glycogen mutant cells had comparably slow P700<sup>+</sup> re-  
3 reduction rate after dark incubation; however, wild type exhibited rapid recovery within 2 hours  
4 in light, while it took 24 hours for the glycogen mutant to reach a comparable level to the wild  
5 type cells (Fig. 3). When comparing between wild type and the  $\Delta gnd$  mutant, the P700<sup>+</sup> re-  
6 reduction rate showed similar trends, i.e. a much faster re-reduction rate in wild type cells after a  
7 short incubation in the light (Fig. 4B). This strongly suggests a higher ATP/NADPH ratio  
8 requirement when photosynthesis first starts and is directly linked to glycogen metabolism and  
9 the OPP pathway. The action of OPP pathway along the Calvin-Benson cycle exacerbates the  
10 deficit of ATP/NADPH ratio needed for carbon fixation(Sharkey and Weise, 2016). It is well  
11 accepted that the additional ATP requirement in photosynthetic carbon metabolism can be  
12 fulfilled through the cyclic electron flow(Kramer and Evans, 2011). The higher CEF rate  
13 observed in the wild type cells fits well with the additional ATP requirements for operating the  
14 OPPP during the start of photosynthesis. Compared to the glycogen mutant, the  $\Delta gnd$  mutant did  
15 not recover to a comparable level of P700<sup>+</sup> re-reduction rate even after 24 hours into the light,  
16 indicating that the OPP pathway is essential for the initiation of photosynthesis and the fitness of  
17 cells (Fig. 4B). When the Calvin-Benson cycle reactions are fully operational (i.e. hours in the  
18 light), the glycogen metabolism and the OPPP might play smaller roles, as revealed by the  
19 similar P700<sup>+</sup> re-reduction rates in light-adapted wild type and glycogen mutant cells (Fig. 3).

20 Glycogen degradation through the OPP pathway could replenish RuBP to ensure the  
21 continuous operation of carbon fixation during the start of photosynthesis. However, it is  
22 important to know that the OPP pathway does not lead to any net carbon fixation. The CO<sub>2</sub> fixed  
23 in the Calvin-Benson cycle is quickly lost when G6P is oxidized to Ru5P in the shunt. It is thus

1 intriguing to understand the role the OPP pathway in supporting photosynthesis. We propose that  
2 the OPP pathway could generate additional NADPH required for the redox regulation of the  
3 Calvin-Benson cycle during the start of photosynthesis. Previous research showed that the  
4 activities of two key enzymes in the Calvin-Benson cycle, PRK and G3P dehydrogenase  
5 (GADPH), are suppressed in dark through the formation of a CP12/PRK/GAPDH protein  
6 complex(Tamoi et al., 2005). The reversible dissociation of the complex was controlled by the  
7 NADP(H)/NAD(H) ratio in *S. elongatus*(Tamoi et al., 2005). The operation of the OPP pathway  
8 during the start of the photosynthesis thus could contribute largely to the increase of NADPH  
9 levels when light resumes, releasing PRK and GAPDH from the complex to activate the Calvin-  
10 Benson cycle. The measurement of reducing equivalents both at the end of dark incubation and  
11 after light was turned on for two hours supports this hypothesis. Compared to the glycogen  
12 mutant  $\Delta glgC$  cells, the increase of NADP(H)/NAD(H) ratio in the wild type was significantly  
13 larger after the light was turned on, i.e. when photosynthesis restarts (Fig. 4C).

14 Lastly, it is also important to understand the activation mechanism of the OPP pathway.  
15 The expression of many genes in the glycogen metabolism and the OPP pathway are controlled  
16 by the circadian clock output protein RpaA(Markson et al., 2013; Welkie et al., 2018). Our  
17 proteomics analysis confirmed that many enzymes in these two metabolic processes were  
18 expressed much higher in wild type cells in the beginning of photosynthesis (Fig. 4A and Table  
19 S1). Previous research also reported that the first enzyme G6P dehydrogenase (G6PDH) in the  
20 OPP pathway is redox regulated and is inactive in its reduced form(Udvardy et al., 1984;  
21 Gleason, 1996). However, G6P could also stabilize and activate G6P dehydrogenase to reverse  
22 the effect of reduction inhibition in cyanobacteria(Cossar et al., 1984). It is thus possible that  
23 glycogen degradation would lead to increased G6P levels and activate the G6P dehydrogenase.

1 Future studies toward understanding these mechanisms could help fully appreciate the roles  
2 played by the OPP pathway in supporting photosynthesis.

3 In conclusion, we found that glycogen metabolism in cyanobacteria could help activate  
4 photosynthesis through the OPP pathway during the start of photosynthesis reactions. The OPP  
5 pathway is generally considered for its role to generate reducing equivalent for dark respiration.  
6 However, evolution empowers cells with the ability to leverage existing metabolic processes to  
7 its advantage in order to adapt to the constantly changing environment. We have witnessed an  
8 interesting strategy implemented by cyanobacteria to ensure their growth advantage in their  
9 natural environment.

## 1 **Materials and Methods**

2 **Growth conditions.** Seed cultures of *S. elongatus* wild type and mutant strains were grown in  
3 BG11 media supplemented with 20 mM sodium bicarbonate and 10 mM N-  
4 [Tris(hydroxymethyl)methyl]-2-aminoethanesulfonic acid (TES, pH 8.2) at 30 °C under 30  $\mu\text{mol}$   
5 photons  $\text{m}^{-2} \text{s}^{-1}$  illumination. The growth media of the mutant strains were also supplemented  
6 with 5 mg/L kanamycin. Cultures for measurements were grown at 30 °C under 50  $\mu\text{mol}$  photons  
7  $\text{m}^{-2} \text{s}^{-1}$  illumination in the Multi-Cultivator MC-1000-OD-MULTI (Photon Systems Instruments,  
8 Czech Republic). Cyanobacterial growth was monitored using the built-in spectrophotometer of  
9 Multi-Cultivator by measuring optical densities at the wavelength of 720 nm.

10 **Plasmid and strain construction.** The gene fragments for plasmid construction were amplified  
11 using primers designed through the NEBuilder Assembly tool (<http://nebuilder.neb.com/>). The  
12 *glgC* and *gnd* knock out plasmids were constructed using HiFi DNA Assembly master mix  
13 (NEB, Ipswich, MA). *S. elongatus* wild type cells were transformed with knockout plasmids to  
14 generate  $\Delta\text{glgC}$  and  $\Delta\text{gnd}$  mutant strains. The strains and plasmids along with primers used in  
15 this study are listed in the supplemental information in Table S2 and S3, and File S1 and S2.

16 **Proteomics Analysis.** Log-phase *S. elongatus* wild type and glycogen mutant cells were used for  
17 proteomics analysis following our previously described method(Wang et al., 2016). For dark-  
18 incubated samples, log-phase cells were taken after light was turned on for two hours following  
19 dark incubation. Briefly, biological triplicates of approximate 10 OD of cells were used for  
20 protein extraction. Cell pellets were resuspended in 1 mL of Tris buffer (50 mM Tris-HCl, 10  
21 mM  $\text{CaCl}_2$ , 0.1 % n-Dodecyl  $\beta$ -D-maltoside, pH 7.6), followed by cell lysis using a homogenizer  
22 with bead-beating cycles of 10 s ON and 2 min OFF on ice for a total of 6 cycles. Protein extract



1 in the supernatant was collected by centrifugation at 13000g for 30 min at 4°C, followed by  
2 protein concentration measurement using the Bradford assay (Thermo Scientific).

3 For each sample, 100 µg of total protein was digested by Trypsin Gold (Promega,  
4 Madison, WI) with 1:100 w/w ratio at 37 °C for 18 hours. The digested peptides were cleaned up  
5 using a Sep-Pak C18 column (Waters Corporation, Milford, MA), followed by peptide  
6 fractionation using the Pierce High pH Reverse-Phase Peptide Fractionation Kit (Thermo  
7 Scientific, Rockford, IL). Eight fractions of peptides from each sample were subjected to liquid  
8 chromatography-tandem mass spectrometry (LC-MS/MS) analysis in a Thermo LTQ Orbitrap  
9 XL mass spectrometer. The mass spec analysis was operated under the data-dependent mode  
10 scanning the mass range of 350-1800  $m/z$  at the resolution of 30,000. The 12 most abundant  
11 peaks were subjected to MS/MS analysis by the collision induced dissociation fragmentation.  
12 The raw data collected from MS/MS analysis was searched and analyzed using the pipeline  
13 programs integrated in the PatternLab for Proteomics (version 4.1.0.17)(Carvalho et al., 2016).  
14 The normalized spectral abundance factor (NSAF) was used to compare protein abundance in  
15 different groups(Zybaylov et al., 2006). The mass spectrometry proteomics data have been  
16 deposited to both the MassIVE repository with the dataset identifier MSV000083575, and the  
17 ProteomeXchange Consortium(Vizcaíno et al., 2015) with the dataset identifier PXD013099.

18 **Photosystem II (PSII) analysis:** Cyanobacterial cells grown both under continuous light (50  
19 µmol photons  $m^{-2} s^{-1}$ ) and dark incubated cells were subjected to PSII measurement using the  
20 Phyto-PAM Phytoplankton Analyzer (Walz, Germany). When measuring PSII efficiency, the  
21 dark adaption that normally oxidizes the PSII center in green algae does not work in *S.*  
22 *elongatus*. Instead, cells would transit to state II after dark adaptation(Campbell et al., 1998). To  
23 get a proper measurement of PSII efficiency, cells were illuminated at moderate actinic light (25

1  $\mu\text{mol}/\text{m}^2/\text{s}$ ) for 5 minutes to lock the photosystems in state I and to oxidize PSII reaction centers.  
2 Standard induction curves by exposing cells to saturation pulses were recorded for the  
3 measurement of the maximum PSII efficiency ( $F_V/F_M$ ) and the effective PSII efficiency ( $\Phi_{II}$ ).  
4 **Photosystem I (PSI) analysis:** Log-phase *S. elongatus* wild type and mutant cells were  
5 incubated in dark for 16 hours before the PSI analysis. Five mL of the culture was vacuum-  
6 filtered through Whatmann GF/C 25 mm filter discs (Cat# 1822-025). Far red light induced P700  
7 oxidation-reduction kinetics measurements were performed using a dual-wavelength pulse  
8 amplitude-modulated fluorescence monitoring system (Dual-PAM-100, Heinz Walz, Effeltrich,  
9 Germany) with a leaf attachment. The proportion of photooxidizable P700 ( $\Delta A_{820}/A_{820}$ ) was  
10 determined as the change in absorbance at 820 nm after turning on the far-red light  
11 ( $\lambda_{\text{max}} = 715 \text{ nm}$ ,  $10 \text{ W m}^{-2}$ , Scott filter RG 715). The half-time for the re-reduction of P700<sup>+</sup> to  
12 P700 ( $t_{1/2}^{\text{red}}$ ) was calculated after the far-red light was turned off and used as an estimate of  
13 alternative electron flow around PSI.

#### 14 **Measurement of NADP(H) and NAD(H) levels.**

15 Log-phase *S. elongatus* wild type and  $\Delta glgC$  cells were incubated in the dark for 16 hours before  
16 the light was turned on. 50  $\mu\text{L}$  of cells were collected in triplicates both at the end of dark  
17 incubation and after the light was on for 2 hours. The levels of pyridine nucleotides NAD(P)<sup>+</sup>  
18 and NAD(P)H were determined by the NAD/NADH-Glo™ and NADP/NADPH-Glo™ assays  
19 (Cat# G9071, Promega, Madison, WI) following the manufacturer's instructions.

#### 20 **Acknowledgements**

21 This work was supported by Miami University startup fund to XW. XW and RMK are also  
22 supported by Department of Energy-BES Photosynthetic Systems program. We thank Drs.  
23 Spencer Diamond, James Golden, and Susan Golden for the original plasmid used to generate the

1 glycogen mutant strain in the preliminary study. We would like to thank Dr. Theresa Ramelot  
2 and Kundi Yang of the chemistry department at Miami University for their help in the  
3 preliminary metabolite analysis. We thank Dr. Jianping Yu (NREL) for the careful reading of the  
4 manuscript.

#### 5 **Author contributions**

6 XW designed and performed the experiment, analyzed data, and wrote the manuscript. SS, SPS,  
7 XZ and IK performed the genetics, proteomics, and photochemistry experiments. RMK helped  
8 analyze the photochemistry data. SS, XL and RMK edited the manuscript.

#### 9 **Competing interests**

10 The authors declare no conflict of interest.

11

1 **References**

- 2 **Bassham JA, Benson AA, Kay LD, Harris AZ, Wilson AT, Calvin M** (1954) The path of  
3 carbon in photosynthesis. XXI. The cyclic regeneration of carbon dioxide acceptor. *J.*  
4 *Am. Chem. Soc.* **76**: 1760-1770
- 5 **Broedel S, Wolf R** (1990) Genetic tagging, cloning, and DNA sequence of the *Synechococcus*  
6 sp. strain PCC 7942 gene (*gnd*) encoding 6-phosphogluconate dehydrogenase. *J Bacteriol*  
7 **172**: 4023-4031
- 8 **Campbell D, Hurry V, Clarke AK, Gustafsson P, Öquist G** (1998) Chlorophyll fluorescence  
9 analysis of cyanobacterial photosynthesis and acclimation. *Microbiol. Mol. Biol. R.* **62**:  
10 667-683
- 11 **Cano M, Holland SC, Artier J, Burnap RL, Ghirardi M, Morgan JA, Yu J** (2018) Glycogen  
12 synthesis and metabolite overflow contribute to energy balancing in cyanobacteria. *Cell*  
13 *Rep.* **23**: 667-672
- 14 **Carvalho PC, Lima DB, Leprevost FV, Santos MD, Fischer JS, Aquino PF, Moresco JJ,**  
15 **Yates III JR, Barbosa VC** (2016) Integrated analysis of shotgun proteomic data with  
16 PatternLab for proteomics 4.0. *Nat. Protoc.* **11**: 102
- 17 **Chen X, Schreiber K, Appel J, Makowka A, Fahrnich B, Roettger M, Hajirezaei MR,**  
18 **Sonnichsen FD, Schonheit P, Martin WF, Gutekunst K** (2016) The Entner-Doudoroff  
19 pathway is an overlooked glycolytic route in cyanobacteria and plants. *Proc. Natl. Acad.*  
20 *Sci. U. S. A.* **113**: 5441-5446
- 21 **Cook G, Teufel A, Kalra I, Li W, Wang X, Priscu J, Morgan-Kiss R** (2019) The Antarctic  
22 psychrophiles *Chlamydomonas* spp. UWO241 and ICE-MDV exhibit differential  
23 restructuring of photosystem I in response to iron. *Photosynth. Res.:* 1-20
- 24 **Cossar JD, Rowell P, Stewart WDP** (1984) Thioredoxin as a modulator of glucose-6-  
25 phosphate-dehydrogenase in a N<sub>2</sub>-fixing cyanobacterium. *J. Gen. Microbiol.* **130**: 991-  
26 998
- 27 **Diamond S, Rubin BE, Shultzaberger RK, Chen Y, Barber CD, Golden SS** (2017) Redox  
28 crisis underlies conditional light–dark lethality in cyanobacterial mutants that lack the  
29 circadian regulator, RpaA. *Proc. Natl. Acad. Sci. U. S. A.* **114**: E580-E589

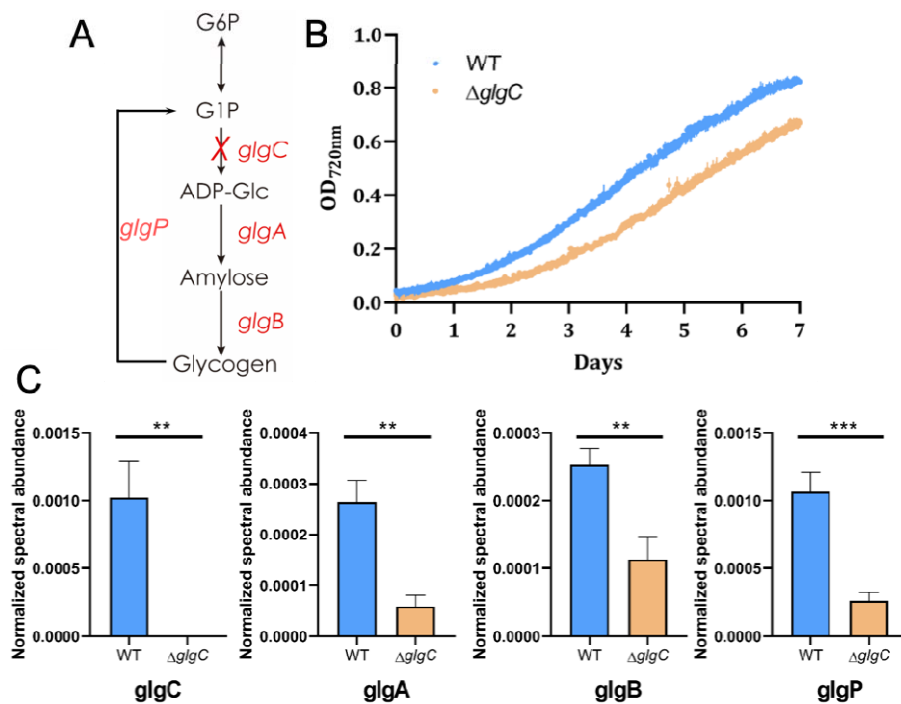
- 1 **Doello S, Klotz A, Makowka A, Gutekunst K, Forchhammer K** (2018) A specific glycogen  
2 mobilization strategy enables rapid awakening of dormant cyanobacteria from chlorosis.  
3 *Plant Physiol* **177**: 594-603
- 4 **Gleason FK** (1996) Glucose-6-phosphate dehydrogenase from the cyanobacterium, *Anabaenasp.*  
5 PCC 7120: purification and kinetics of redox modulation. *Arch. Biochem. Biophys.* **334**:  
6 277-283
- 7 **Gomez-Casati DF, Cortassa S, Aon MA, Iglesias AA** (2003) Ultrasensitive behavior in the  
8 synthesis of storage polysaccharides in cyanobacteria. *Planta* **216**: 969-975
- 9 **Harrison EP, Olcer H, Lloyd JC, Long SP, Raines CA** (2001) Small decreases in SBPase  
10 cause a linear decline in the apparent RuBP regeneration rate, but do not affect Rubisco  
11 carboxylation capacity. *J Exp Bot* **52**: 1779-1784
- 12 **Harrison EP, Willingham NM, Lloyd JC, Raines CA** (1997) Reduced sedoheptulose-1, 7-  
13 biphosphatase levels in transgenic tobacco lead to decreased photosynthetic capacity and  
14 altered carbohydrate accumulation. *Planta* **204**: 27-36
- 15 **Holland SC, Artier J, Miller NT, Cano M, Yu JP, Ghirardi ML, Burnapa RL** (2016)  
16 Impacts of genetically engineered alterations in carbon sink pathways on photosynthetic  
17 performance. *Algal Res.* **20**: 87-99
- 18 **Iijima H, Shirai T, Okamoto M, Kondo A, Hirai MY, Osanai T** (2015) Changes in primary  
19 metabolism under light and dark conditions in response to overproduction of a response  
20 regulator RpaA in the unicellular cyanobacterium *Synechocystis* sp. PCC 6803. *Front.*  
21 *Microbiol.* **6**: 888
- 22 **Klughammer C, Schreiber U** (1994) An improved method, using saturating light pulses, for the  
23 determination of photosystem I quantum yield via P700+-absorbance changes at 830 nm.  
24 *Planta* **192**: 261-268
- 25 **Knowles VL, Plaxton WC** (2003) From genome to enzyme: analysis of key glycolytic and  
26 oxidative pentose-phosphate pathway enzymes in the cyanobacterium *Synechocystis* sp.  
27 PCC 6803. *Plant Cell Physiol.* **44**: 758-763
- 28 **Kramer DM, Evans JR** (2011) The importance of energy balance in improving photosynthetic  
29 productivity. *Plant Physiol* **155**: 70-78
- 30 **Lehmann M, Wöber G** (1976) Accumulation, mobilization and turn-over of glycogen in the  
31 blue-green bacterium *Anacystis nidulans*. *Arch Microbiol* **111**: 93-97

- 1 **Li J, Weraduwege SM, Preiser AL, Weise SE, Strand DD, Froehlich JE, Kramer DM, Hu**  
2 **J, Sharkey TD** (2018) Loss of peroxisomal hydroxypyruvate reductase inhibits triose  
3 phosphate isomerase but stimulates cyclic photosynthetic electron flow and the glc-6P-  
4 phosphate shunt. bioRxiv
- 5 **Markson JS, Piechura JR, Puszynska AM, O'Shea EK** (2013) Circadian control of global  
6 gene expression by the cyanobacterial master regulator RpaA. *Cell* **155**: 1396-1408
- 7 **Mullineaux CW** (2014) Co-existence of photosynthetic and respiratory activities in  
8 cyanobacterial thylakoid membranes. *Biochim. Biophys. Acta Bioenerg.* **1837**: 503-511
- 9 **Preiser AL, Banerjee A, Fisher N, Sharkey TD** (2018) Supply and consumption of glucose 6-  
10 phosphate in the chloroplast stroma. bioRxiv: 442434
- 11 **Preiss J** (1984) Bacterial glycogen synthesis and its regulation. *Annu. Rev. Microbiol.* **38**: 419-  
12 458
- 13 **Puszynska AM, O'Shea EK** (2017) Switching of metabolic programs in response to light  
14 availability is an essential function of the cyanobacterial circadian output pathway. *Elife*  
15 **6**: e23210
- 16 **Raines CA, Lloyd JC, Dyer TA** (1999) New insights into the structure and function of  
17 sedoheptulose-1, 7-bisphosphatase; an important but neglected Calvin cycle enzyme. *J*  
18 *Exp Bot* **50**: 1-8
- 19 **Scanlan DJ, Sundaram S, Newman J, Mann NH, Carr NG** (1995) Characterization of a *zwf*  
20 mutant of *Synechococcus* sp. strain PCC 7942. *J Bacteriol* **177**: 2550-2553
- 21 **Sharkey TD, Weise SE** (2016) The glucose 6-phosphate shunt around the Calvin-Benson cycle.  
22 *J Exp Bot* **67**: 4067-4077
- 23 **Shimakawa G, Hasunuma T, Kondo A, Matsuda M, Makino A, Miyake C** (2014)  
24 Respiration accumulates Calvin cycle intermediates for the rapid start of photosynthesis  
25 in *Synechocystis* sp. PCC 6803. *Biosci. Biotechnol. Biochem.* **78**: 1997-2007
- 26 **Smith A** (1983) Modes of cyanobacterial carbon metabolism. *Ann. Inst. Pasteur Microbiol.* **134**:  
27 93-113
- 28 **Suzuki E, Ohkawa H, Moriya K, Matsubara T, Nagaike Y, Iwasaki I, Fujiwara S, Tsuzuki**  
29 **M, Nakamura Y** (2010) Carbohydrate metabolism in mutants of the cyanobacterium  
30 *Synechococcus elongatus* PCC 7942 defective in glycogen synthesis. *Appl. Environ.*  
31 *Microbiol.* **76**: 3153-3159

- 1 **Tamoi M, Miyazaki T, Fukamizo T, Shigeoka S** (2005) The Calvin cycle in cyanobacteria is  
2 regulated by CP12 via the NAD(H)/NADP(H) ratio under light/dark conditions. *Plant J*  
3 **42**: 504-513
- 4 **Udvardy J, Borbely G, Juhász A, Farkas GL** (1984) Thioredoxins and the redox modulation  
5 of glucose-6-phosphate dehydrogenase in *Anabaena* sp. strain PCC 7120 vegetative cells  
6 and heterocysts. *J Bacteriol* **157**: 681-683
- 7 **Vizcaino JA, Csordas A, Del-Toro N, Dianas JA, Griss J, Lavidas I, Mayer G, Perez-**  
8 **Riverol Y, Reisinger F, Ternent T** (2015) 2016 update of the PRIDE database and its  
9 related tools. *Nucleic Acids Res* **44**: D447-D456
- 10 **Wang X, Liu W, Xin C, Zheng Y, Cheng Y, Sun S, Li R, Zhu XG, Dai SY, Rentzepis PM,**  
11 **Yuan JS** (2016) Enhanced limonene production in cyanobacteria reveals photosynthesis  
12 limitations. *Proc. Natl. Acad. Sci. U. S. A.* **113**: 14225-14230
- 13 **Welkie DG, Rubin BE, Chang Y-G, Diamond S, Rifkin SA, LiWang A, Golden SS** (2018)  
14 Genome-wide fitness assessment during diurnal growth reveals an expanded role of the  
15 cyanobacterial circadian clock protein KaiA. *Proc. Natl. Acad. Sci. U. S. A.* **115**: E7174-  
16 E7183
- 17 **Welkie DG, Rubin BE, Diamond S, Hood RD, Savage DF, Golden SS** (2018) A hard day's  
18 night: Cyanobacteria in diel cycles. *Trends in microbiology*
- 19 **Xu Q, Yu L, Chitnis VP, Chitnis PR** (1994) Function and organization of photosystem I in a  
20 cyanobacterial mutant strain that lacks PsaF and PsaJ subunits. *J Biol Chem* **269**: 3205-  
21 3211
- 22 **Zybailov B, Mosley AL, Sardiù ME, Coleman MK, Florens L, Washburn MP** (2006)  
23 Statistical analysis of membrane proteome expression changes in *Saccharomyces c*  
24 *erevisiae*. *J. Proteome. Res.* **5**: 2339-2347

25  
26

1 **Fig. 1. Impact of glycogen metabolism on *S. elongatus* growth.** (A) Glycogen synthesis  
2 pathway in *S. elongatus*. The gene *glgC* was deleted from *S. elongatus* genome to create the  
3 glycogen mutant. (B) Growth curves of *S. elongatus* wild type and glycogen mutant cells  
4 ( $\Delta glgC$ ) measured by density optical at 720 nm. (C) Comparative proteomics analysis of *S.*  
5 *elongatus* wild type and glycogen mutant cells. Enzymes for both glycogen biosynthesis  
6 (AGPase (*glgC*), GS (*glgA*) and 1,4-alpha-glucan branching enzyme (*glgB*)) and degradation  
7 (alpha-1,4-glucan phosphorylase (*glgP*)) were highly expressed in wild type compared to  
8 glycogen mutant cells. Bar graph indicates enzyme expression levels based on the normalized  
9 spectral abundance factor (NSAF) (\* $p < 0.05$ , \*\* $p < 0.01$ , \*\*\* $p < 0.001$ ).



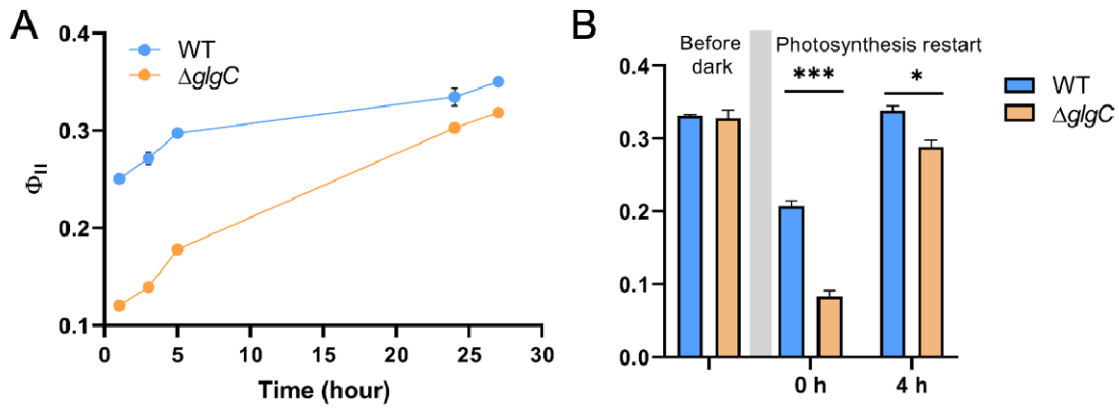
10

11



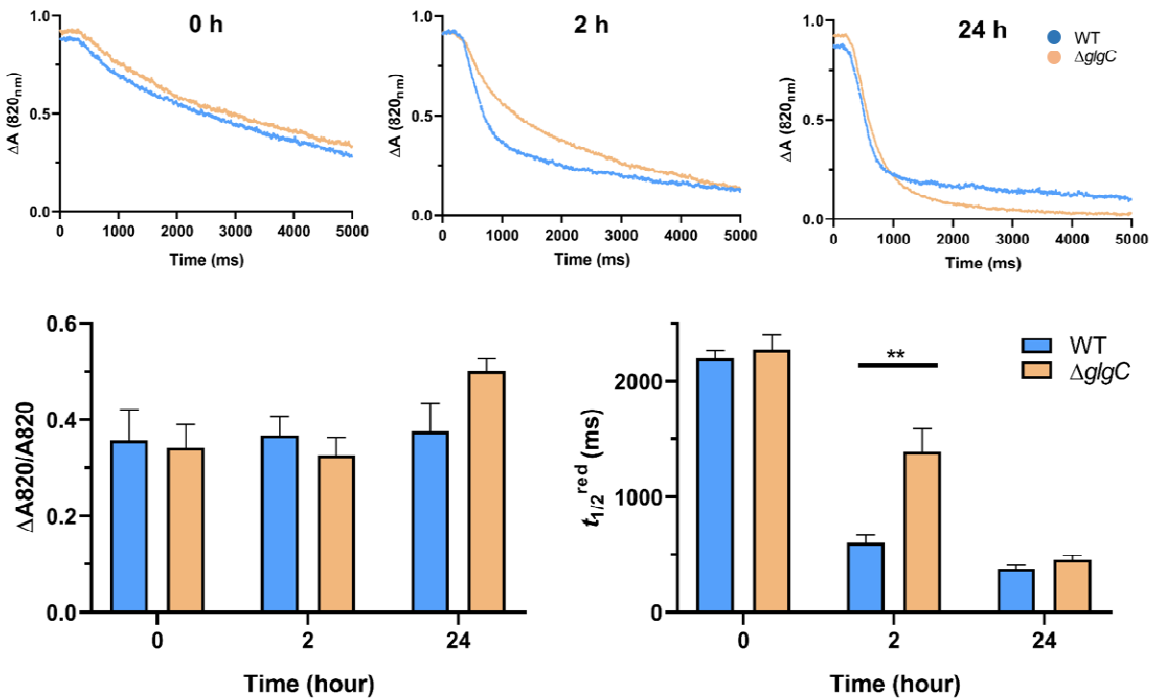
1 **Fig. 2. Photosystem II (PSII) efficiency of *S. elongatus* wild type and glycogen mutant cells.**

2 (A) The effective PSII efficiency ( $\Phi_{II}$ ) measured under continuous light. Paired t test showed a p  
3 value of 0.0193 between wild type and glycogen mutant. (B) The effective PSII efficiency ( $\Phi_{II}$ )  
4 in dark incubated cells. Both  $\Phi_{II}$  following the dark incubation (0 h) and after light was turned on  
5 for 4 hours were measured to monitor the effective PSII efficiency during photosynthesis restart.  
6 (\*p<0.05, \*\*\*p<0.001)



7  
8

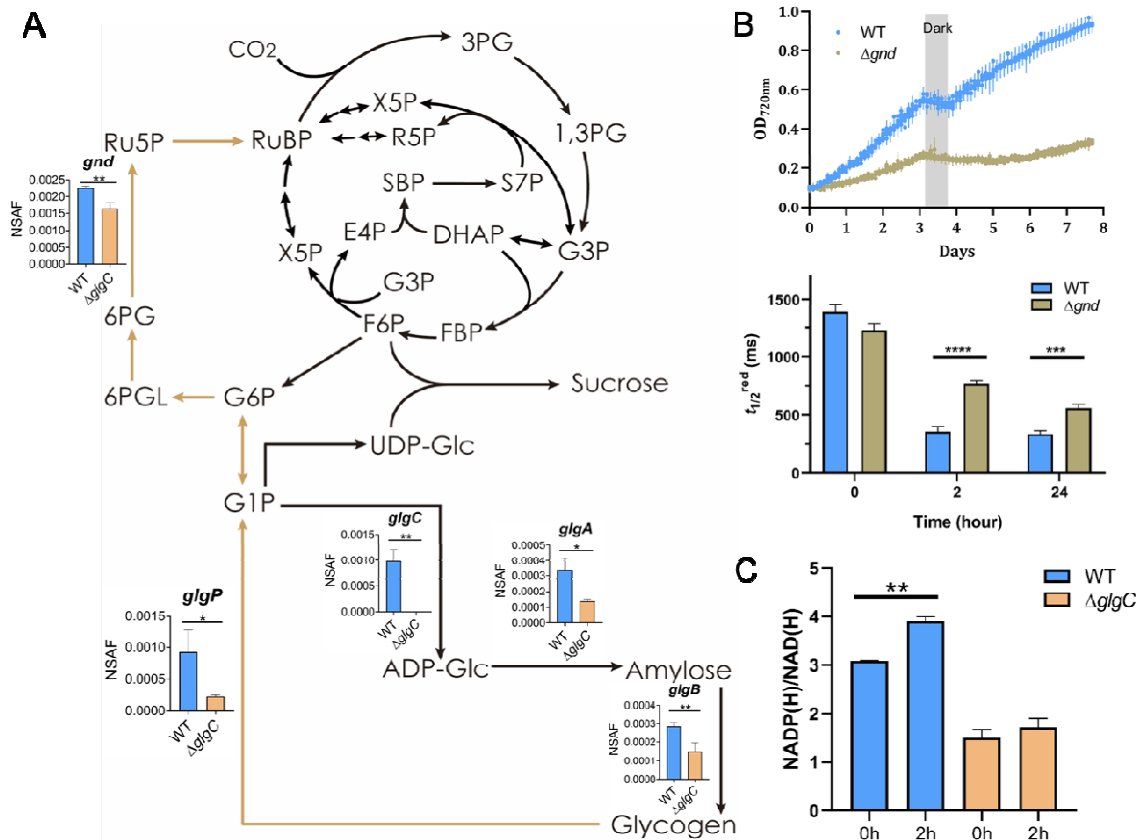
1 **Fig. 3. P700<sup>+</sup> reduction in *S. elongatus* wild type and glycogen mutant cells following dark**  
2 **incubation.** Cultures were incubated in the dark for 16 hours. The P700<sup>+</sup> reduction was  
3 measured right after dark adaption (0 h), 2 hours into the light (2 h), and 24 hours into the light  
4 (24 h). The data was plotted from the means of 9 replicates (3 biological × 3 technical  
5 replicates). Bar graphs indicate the oxidizable P700 pool ( $\Delta A_{820}/A_{820}$ ) and the calculated  
6 P700<sup>+</sup> re-reduction rate ( $t_{1/2}^{\text{red}}$ ) from the slope of the reduction curve. (\*\*p<0.01).



7

8

1 **Fig. 4. Glycogen metabolism jump-starts photosynthesis through the OPPP.** (A) Yellow  
 2 arrows indicate the proposed mechanism in which glycogen degrades through the OPPP to  
 3 recharge photosynthesis during the start of photosynthesis. Bar graphs indicate the protein levels  
 4 from proteomics analysis. (B) Growth profile and P700<sup>+</sup> re-reduction analysis of wild type and  
 5 the OPP pathway mutant  $\Delta gnd$ . Bar graph indicates the calculated P700<sup>+</sup> re-reduction rate ( $t_{1/2}^{red}$ ).  
 6 (C) Detection of NADP(H)/NAD(H) ratio in both wild type and glycogen mutant  $\Delta glgC$  cells  
 7 following dark incubation and after 2 hours into the light. (\* $p < 0.05$ , \*\* $p < 0.01$ , \*\*\* $p < 0.001$ ).  
 8 (Relevant acronyms: **3PG**: 3-phosphoglycerate; **G3P**: Glyceraldehyde 3-phosphate; **Ru5P**:  
 9 Ribulose 5-phosphate; **RuBP**: Ribulose 1,5-bisphosphate; **G6P**: Glucose 6-phosphate; **6PGL**: 6-  
 10 phosphogluconolactone; **G1P**: Glucose 1-phosphate; **ADP-Glc**: ADP-glucose.)



11

12